ACS APPLIED MATERIALS & INTERFACES

Letter

www.acsami.org

Ag_2Se Quantum Dots with Tunable Emission in the Second Near-Infrared Window

Chun-Nan Zhu,[†,‡] Peng Jiang,[†,‡] Zhi-Ling Zhang,[†,‡] Dong-Liang Zhu,[†,‡] Zhi-Quan Tian,*[,†,‡,§] and Dai-Wen Pang[†,‡]

[†]Key Laboratory of Analytical Chemistry for Biology and Medicine (Ministry of Education), College of Chemistry and Molecular Sciences, and State Key Laboratory of Virology, Wuhan University, Wuhan 430072, P. R. China

[‡]Wuhan Institute of Biotechnology, Wuhan 430075, P. R. China

[§]Research Center of Ion Beam Application in Functional Materials, Wuhan University, Wuhan 430072, P. R. China

Supporting Information

ABSTRACT: Quantum dots (QDs) with fluorescence in the second near-infrared window (NIR-II, 1000−1400 nm) are ideal fluorophores for in vivo imaging of deep tissue with high signal-to-noise ratios. Ag_2Se (bulk band gap 0.15 eV) is a promising candidate for preparing NIR-II QDs. By using 1-octanethiol as ligand to effectively balance the nucleation and growth, tuning the fluorescence of Ag_2Se QDs was successfully realized in the NIR-II window ranged from 1080 to 1330 nm. The prepared Ag_2Se QDs can be conveniently transferred to the aqueous phase by ligand exchange, showing great potential for multicolor NIR-II fluorescence imaging in vivo.

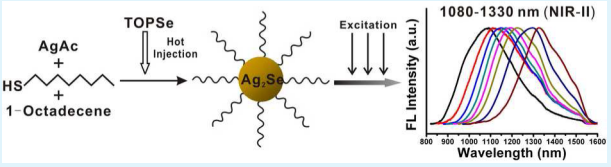

KEYWORDS: *Ag_2Se, quantum dots, fluorescence, second near-infrared window, tunable emission*

Near-infrared fluorescence penetrates deep in the body, and is less interfered by the scattering, absorption and autofluorescence of tissue and blood, which make it favorable for in vivo imaging.[1,2] Especially, fluorescence in the second near-infrared window (NIR-II, 1000−1400 nm) has higher penetration depth than that in NIR-I (750−900 nm) and could image deep tissue with high signal-to-noise ratios.[3,4] Quantum dots (QDs) have been promising labels for fluorescence imaging in biomedicine due to their unique optical properties.[5,6] Possessing the advantages of both QDs and NIR-II fluorescence, QDs with emission in NIR-II (NIR-II QDs) are ideal fluorophores for in vivo imaging and have drawn much attention in the past decade.[7,8] However, most of the studied NIR-II QDs (CdHgTe, PbS, PbSe, and PbTe)[9−12] contained the toxic element Cd, Hg or Pb, which limited their in vivo applications.

Silver chalcogenides, which have low toxicity and narrow band gaps (0.9 eV for bulk Ag_2S, 0.15 eV for Ag_2Se, and 0.67 eV for Ag_2Te),[13−16] have been reported as candidates for NIR-II QDs in recent years. Ag_2S QDs emitting at approximately 1200 nm were prepared[17−19] and applied for in vivo imaging.[7,8] Likewise, attempt has been made to prepare Ag_2Se nanoparticles (NPs). Nonfluorescent Ag_2Se,[20−22] NIR-II Ag_2Se QDs[23] and small-sized water-soluble NIR-I Ag_2Se QDs[24] were successfully synthesized. However, it is still a challenge to conveniently tune the emission of Ag_2Se QDs in the second near-infrared window, which is necessary to realize multicolor labeling to synchronously image multiple targets with high signal-to-noise ratios. Herein, we report the synthesis of fluorescence-tunable NIR-II Ag_2Se QDs by varying the reaction time with the appropriate ligand.

In the synthesis of Ag_2Se QDs, silver acetate (AgAc), the ligand and 1-octadecene (ODE) were mixed in a three-neck flask under argon flow. TOPSe (Se dissolved in tri-n-octylphosphine (TOP)) was quickly injected into the hot reaction mixture at the elevated temperature. The resulting products were dispersed in nonpolar solvents for further measurements. As known to us, ligands play an important role in the nucleation and growth of nanoparticles.[25,26] To prepare high-quality Ag_2Se QDs with tunable fluorescence (FL) in the NIR-II window, we investigated various common used ligands, including oleylamine (OAm), tetradecylphosphonic acid (TDPA) and 1-octanethiol, to find the appropriate ligand to modulate FL properties of Ag_2Se QDs.

With OAm or TDPA as ligand, the nonuniform products were easily formed (see Figure S1 and S2 in the Supporting Information). Ag(I) is a very soft Lewis acid, whereas OAm and TDPA are hard Lewis base ligands. These ligands are bound to Ag(I) through weak interactions. When reducing OAm was employed, the synthesis was carried out at a relative low temperature (120 °C) to avoid the formation of Ag NPs. The relative low reaction temperature resulted in low effective monomer concentration,[25] which meant that only a small amount of monomers were used in the initial nucleation stage and excess monomers were left for growth. In addition, the

Received: December 23, 2012
Accepted: February 4, 2013
Published: February 4, 2013

weak binding of OAm to Ag(I) gave rise to quick escape of ligands from the surface of nanoparticles and a rapid growth process. Thus, it was difficult to control the sizes and size distributions of nanoparticles. With nonreducing TDPA as ligand, the effective monomer concentration increased at the relative high reaction temperature (170 °C) due to weak coordinating of TDPA with Ag(I). A large number of monomers were consumed to nucleate and the residual monomers were not sufficient for the further growth. Ostwald ripening and shape evolution underwent with increased reaction time.[26] Therefore, OAm and TDPA were not appropriate ligands to prepare high-quality Ag_2Se NPs.

Using 1-octanethiol, a soft Lewis base ligand, Ag(I) can be effectively stabilized under 180 °C, above which Ag(I) would react with the thiol to form Ag_2S. According to the principle of hard and soft acids and bases (HSAB), there should be a stronger bond between Se and Ag(I) than S and Ag(I). Thus, the Ag−S bonds between Ag(I) and 1-octanethiol would break to form Ag−Se bonds when TOPSe was injected. Meanwhile, the appropriate binding of 1-octanethiol to Ag(I) could effectively balance nucleation and growth to obtain high-quality Ag_2Se NPs. Accordingly, we designed a synthetic route (Scheme 1) to prepare NIR Ag_2Se QDs. The experimental details were described in the Supporting Information.

Scheme 1. Strategy for Preparing Ag_2Se QDs with Tunable Emission in the Second Near-Infrared Window

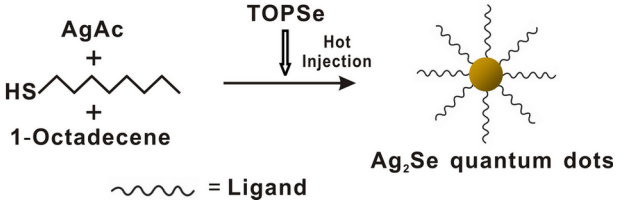

Transmission electron microscopy (TEM) images displayed that the products obtained at different reaction times were spherical particles with good size distributions (Figure 1A, D, G). The particles with sizes of 3.1 ± 0.7 nm, 3.4 ± 0.9 nm and 3.9 ± 0.7 nm (300 particles measured in each image) were obtained at the reaction time of 1 min, 5 min and 1 h, respectively. Powder X-ray diffraction (XRD) pattern (see Figure S3 in the Supporting Information) showed that the diffraction peaks of the products matched with orthorhombic Ag_2Se (JCPDS Card No. 24−1041). The broadened peaks may be attributed to the low crystallinity of small-sized particles. The crystal structure of the products was further confirmed by high-resolution TEM (HRTEM) images (Figure 1B, E, H, and Figure S4 in the Supporting Information). The interplanar spacing of 0.246 nm in Figure 1B, E, and H was consistent with the (013) lattice distance of orthorhombic Ag_2Se. The consistence of calculated and measured interplanar angles of 2-dimension lattice planes in Figure S4 in the Supporting Information further confirmed that as-prepared Ag_2Se QDs were orthorhombic-structured (see Table S1 in the Supporting Information). Energy-dispersive X-ray (EDX) result (see Figure S5 in the Supporting Information) showed that the purified products contained Ag and Se elements with an approximate atomic ratio of 1.87:1.00, close to the stoichiometry of Ag_2Se. Meanwhile, EDX also exhibited the peak of element S, which may arise from the ligand 1-octanethiol used in the synthesis. X-ray photoelectron spectroscopy (XPS) data (see Figure S6A in the Supporting Information) suggested that elemental Ag and Se were present in the purified products. The high-resolution XPS spectra of Ag 3d and Se 3d (see Figure S6B, C in the Supporting Information) showed binding energies of 368.0 eV, 374.0 eV, and 53.9 eV that could respectively correspond to Ag $3d_{5/2}$, Ag $3d_{3/2}$ and Se 3d.[20] The high-resolution XPS spectrum of S 2p showed binding energy of 162.0 eV, indicating the presence of bound thiolate (see Figure S6D in the Supporting Information).[27−29] Characteristic peaks of alkane were observed and no peak of free thiols existed in Fourier transform infrared (FT-IR) spectrum (see Figure S7 in the Supporting Information). Thus, it could be concluded that the products were Ag_2Se QDs capped with 1-octanethiol.

UV−vis−NIR and fluorescence spectrophotometers were employed to characterize optical properties of the as-prepared Ag_2Se QDs. With increased reaction time, Ag_2Se QDs displayed red-shift absorption in the range from 770 to 1070 nm and red-shift FL emission in the range from 1080 to 1330 nm (Figure 2A, B). Using organic dye ICG in dimethyl sulfoxide ($\Phi \approx 0.13$) as standard, FL quantum yields (QY) of Ag_2Se QDs were measured to be up to 9.58%. Replotted in the "Tauc plot" format, absorption spectra can be used to calculate optical band gaps of quantum dots. The Ag_2Se QDs with reaction time of 1

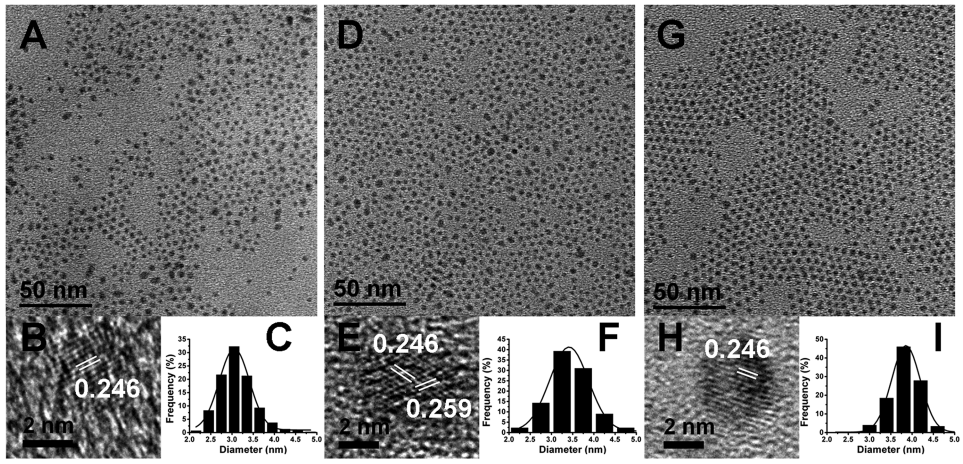

Figure 1. TEM images of Ag_2Se QDs with different reaction times: (A) 1 min, (D) 5 min, (G) 1 h; (B, E, H) the corresponding HRTEM images and (C, F, I) size histograms.

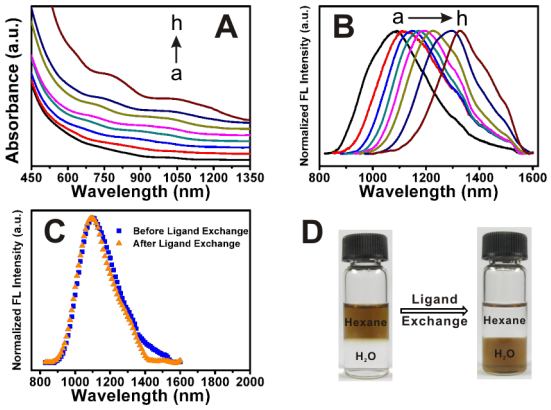

Figure 2. (A) Absorption and (B) FL emission spectra of the as-prepared Ag_2Se QDs with different reaction times: (a) 5 s, (b) 1 min, (c) 5 min, (d) 10 min, (e) 20 min, (f) 30 min, (g) 45 min, (h) 1 h. (C) FL emission spectra and (D) pictures of Ag_2Se QDs emitting at 1090 nm before/after ligand exchange.

min (a), 5 min (b), and 1 h (c) displayed absorption shoulders at 808 nm, 868 nm, and 1070 nm (see Figure S8 in the Supporting Information), respectively. The corresponding band gaps obtained from Tauc plots of $(\alpha h\nu)^{1/2}$ vs $h\nu$ were 1.54, 1.41, and 1.13 eV, respectively. Meanwhile, the particle sizes can be calculated using the following equation.[30]

$$E_g(\text{dot}) = E_g(\text{bulk}) + \frac{\hbar^2\pi^2}{2R^2}\left(\frac{1}{m_e^*} + \frac{1}{m_h^*}\right) \quad (1)$$

Where, E_g(bulk) and R are representative of the band gap of the bulk material and the particle radius. m_e^* and m_h^* are the electron and hole effective masses. For the orthorhombic Ag_2Se, E_g(bulk) is 0.15 eV, m_e^* is 0.12 m, and m_h^* is 0.75 m.[30−32] The calculated particle sizes of the above three typical Ag_2Se QDs were 3.2, 3.4, and 3.8 nm, respectively, which matched well with the TEM results (Figure 1A, D, and G) (Table 1), indicating that red shifts of absorption of Ag_2Se QDs were related to quantum size effect.

Table 1. Comparison of Sizes of Ag_2Se QDs Obtained from Absorption Spectra and Those Measured by TEM

sample	absorption shoulder (nm)	band gap[a] (eV)	calculated size[b] (nm)	size measured by TEM (nm)
a	808	1.54	3.2	3.1
b	868	1.41	3.4	3.4
c	1070	1.13	3.8	3.9

[a]The band gaps were obtained from absorption spectra replotted in the "Tauc plot" format. [b]The sizes were calculated by eq1.

To investigate the potential of the as-prepared Ag_2Se QDs for biological applications, 11-mercaptoundecanoic acid was employed to transfer Ag_2Se QDs to the aqueous phase by ligand exchange.[18,33,34] After phase transfer, Ag_2Se QDs could be well dispersed in water (see Figure S9 in the Supporting Information) and retain excellent fluorescence properties with QY up to 3.33% (Figure 2C, D and Figure S10 in the Supporting Information), which were favorable for practical application in bioimaging.

In conclusion, Ag_2Se QDs with tunable FL emission in the second near-infrared window (1000−1400 nm) have been synthesized by effectively balancing the nucleation and growth using 1-octanethiol, a soft Lewis base, as ligand. The obtained Ag_2Se QDs showed size-dependent absorption and tunable NIR-II fluorescence in the range from 1080 to 1330 nm. After transferred to the aqueous phase, Ag_2Se QDs still retained excellent fluorescence properties, which was important for their potential applications in the field of multicolor fluorescence imaging in vivo.

■ ASSOCIATED CONTENT

Supporting Information

Experimental details, XRD, EDX, XPS, FT-IR of Ag_2Se QDs. TEM images of Ag_2Se NPs with OAm or TDPA as ligand. FL spectra of Ag_2Se QDs before/after ligand exchange. This material is available free of charge via the Internet at http://pubs.acs.org.

■ AUTHOR INFORMATION

Corresponding Author

*E-mail: zqtian@whu.edu.cn.

Notes

The authors declare no competing financial interest.

■ ACKNOWLEDGMENTS

This work was supported by the National Basic Research Program of China (973 Program, 2011CB933600), the Science Fund for Creative Research Groups of NSFC (No. 20921062), the National Natural Science Foundation of China (21005056 and 21175100), the Program for New Century Excellent Talents in University (NCET-10-0656), Science and Technology Program of Hubei Province (2011BCB013), and the "3551 Talent Program" of the Administrative Committee of East Lake Hi-Tech Development Zone (Grant [2011]137). The authors thank Center for Electron Microscopy (Wuhan University) for acquiring TEM data.

■ REFERENCES

(1) Weissleder, R. *Nat. Biotechnol.* **2001**, *19*, 316−317.
(2) Robinson, J. T.; Hong, G. S.; Liang, Y. Y.; Zhang, B.; Yaghi, O. K.; Dai, H. J. *J. Am. Chem. Soc.* **2012**, *134*, 10664−10669.
(3) Lim, Y. T.; Kim, S.; Nakayama, A.; Stott, N. E.; Bawendi, M. G.; Frangioni, J. V. *Mol. Imaging* **2003**, *2*, 50−64.
(4) Smith, A. M.; Mancini, M. C.; Nie, S. M. *Nat. Nanotechnol.* **2009**, *4*, 710−711.
(5) Chan, W. C. W.; Nie, S. M. *Science* **1998**, *281*, 2016−2018.
(6) Michalet, X.; Pinaud, F. F.; Bentolila, L. A.; Tsay, J. M.; Doose, S.; Li, J. J.; Sundaresan, G.; Wu, A. M.; Gambhir, S. S.; Weiss, S. *Science* **2005**, *307*, 538−544.
(7) Zhang, Y.; Hong, G. S.; Zhang, Y. J.; Chen, G. C.; Li, F.; Dai, H. J.; Wang, Q. B. *ACS Nano* **2012**, *6*, 3695−3702.
(8) Hong, G. S.; Robinson, J. T.; Zhang, Y. J.; Diao, S.; Antaris, A. L.; Wang, Q. B.; Dai, H. J. *Angew. Chem., Int. Ed.* **2012**, *51*, 9818−9821.
(9) Sun, H. Z.; Zhang, H.; Ju, J.; Zhang, J. H.; Qian, G.; Wang, C. L.; Yang, B.; Wang, Z. Y. *Chem. Mater.* **2008**, *20*, 6764−6769.
(10) Moreels, I.; Justo, Y.; De Geyter, B.; Haustraete, K.; Martins, J. C.; Hens, Z. *ACS Nano* **2011**, *5*, 2004−2012.
(11) Du, H.; Chen, C. L.; Krishnan, R.; Krauss, T. D.; Harbold, J. M.; Wise, F. W.; Thomas, M. G.; Silcox, J. *Nano Lett.* **2002**, *2*, 1321−1324.
(12) Murphy, J. E.; Beard, M. C.; Norman, A. G.; Ahrenkiel, S. P.; Johnson, J. C.; Yu, P. R.; Mićić, O. I.; Ellingson, R. J.; Nozik, A. J. *J. Am. Chem. Soc.* **2006**, *128*, 3241−3247.
(13) Meherzi-Maghraoui, H.; Dachraoui, M.; Belgacem, S.; Buhre, K. D.; Kunst, R.; Cowache, P.; Lincot, D. *Thin Solid Films* **1996**, *288*, 217−223.
(14) Khanna, P. K.; Das, B. K. *Mater. Lett.* **2004**, *58*, 1030−1034.
(15) Appel, J. *Z. Naturforsch.* **1955**, *10a*, 530−541.

(16) Ma, X. H.; Zhao, Y. Y.; Jiang, X. Y.; Liu, W.; Liu, S. Q.; Tang, Z. Y. *Chemphyschem* **2012**, *13*, 2531−2535.
(17) Du, Y. P.; Xu, B.; Fu, T.; Cai, M.; Li, F.; Zhang, Y.; Wang, Q. B. *J. Am. Chem. Soc.* **2010**, *132*, 1470−1471.
(18) Jiang, P.; Tian, Z. Q.; Zhu, C. N.; Zhang, Z. L.; Pang, D. W. *Chem. Mater.* **2012**, *24*, 3−5.
(19) Jiang, P.; Zhu, C. N.; Zhang, Z. L.; Tian, Z. Q.; Pang, D. W. *Biomaterials* **2012**, *33*, 5130−5135.
(20) Ge, J. P.; Xu, S.; Liu, L. P.; Li, Y. D. *Chem.—Eur. J.* **2006**, *12*, 3672−3677.
(21) Wang, D. S.; Xie, T.; Peng, Q.; Li, Y. D. *J. Am. Chem. Soc.* **2008**, *130*, 4016−4022.
(22) Sahu, A.; Qi, L. J.; Kang, M. S.; Deng, D. N.; Norris, D. J. *J. Am. Chem. Soc.* **2011**, *133*, 6509−6512.
(23) Yarema, M.; Pichler, S.; Sytnyk, M.; Seyrkammer, R.; Lechner, R. T.; Fritz-Popovski, G.; Jarzab, D.; Szendrei, K.; Resel, R.; Korovyanko, O.; Loi, M. A.; Paris, O.; Hesser, G.; Heiss, W. *ACS Nano* **2011**, *5*, 3758−3765.
(24) Gu, Y. P.; Cui, R.; Zhang, Z. L.; Xie, Z. X.; Pang, D. W. *J. Am. Chem. Soc.* **2012**, *134*, 79−82.
(25) Yu, W. W.; Wang, Y. A.; Peng, X. G. *Chem. Mater.* **2003**, *15*, 4300−4308.
(26) Yu, W. W.; Peng, X. G. *Angew. Chem., Int. Ed.* **2002**, *41*, 2368−2371.
(27) Castner, D. G.; Hinds, K.; Grainger, D. W. *Langmuir* **1996**, *12*, 5083−5086.
(28) Yam, C. M.; Cho, J.; Cai, C. Z. *Langmuir* **2003**, *19*, 6862−6868.
(29) Bao, H. B.; Gong, Y. J.; Li, Z.; Gao, M. Y. *Chem. Mater.* **2004**, *16*, 3853−3859.
(30) Praharaj, S.; Nath, S.; Panigrahi, S.; Basu, S.; Ghosh, S. K.; Pande, S.; Jana, S.; Pal, T. *Chem. Commun.* **2006**, 3836−3838.
(31) Damodara Das, V.; Karunakaran, D. *J. Appl. Phys.* **1990**, *67*, 878−883.
(32) Sahu, A.; Khare, A.; Deng, D. D.; Norris, D. J. *Chem. Commun.* **2012**, *48*, 5458−5460.
(33) Liu, X. F.; Gao, Y.; Wang, X. M.; Wu, S. J.; Tang, Z. Y. *J. Nanosci. Nanotechnol.* **2011**, *11*, 1941−1949.
(34) Qin, B.; Zhao, Z. Z.; Song, R.; Shanbhag, S.; Tang, Z. Y. *Angew. Chem., Int. Ed.* **2008**, *47*, 9875−9878.